

Time-varying non linear modeling of electrodynamic loudspeakers

R. Ravaud ^a, G. Lemarquand ^{a,*} and T. Roussel

^a*Laboratoire d'Acoustique de l'Universite du Maine, UMR CNRS 6613, Avenue
Olivier Messiaen, 72085 Le Mans Cedex 9, France*

Abstract

This paper deals with the time-varying nonlinear analytical modeling of the electrodynamic loudspeaker. We propose a model which takes into account the variations of Small signal parameters. The six Small signal parameters (R_e , L_e , Bl , R_{ms} , M_{ms} , C_{ms}) depend on both time and input current. The electrodynamic loudspeaker is characterized by the electrical impedance which, precisely measured, allows us to construct polynomial functions for each Small signal parameter. By using this analytical model, we propose to compare two identical electrodynamic loudspeakers. One of them is supposed to be run in and the other one is not. The experimental methodology is based on a precise measurement. In all the paper, the time scale is assumed to be much longer than one period of the harmonic excitation.

Key words: Loudspeaker, Electrodynamic, Electrical Impedance

PACS: 43-38 Ja

* Corresponding author.

Email address: `guy.lemarquand@univ-lemans.fr` (G. Lemarquand).

1 Introduction

The reference model describing the electrodynamic loudspeaker designed by Thiele and Small [1] predicts that the electrodynamic loudspeaker is both a linear system and a stationary one. This analytical model is very useful since it is simple to use. However, an electrodynamic loudspeaker exhibits nonlinearities which depend on time. Some authors, such as A.J.M Kaiser [2] and W.Klippel [3] [4], have studied the nonlinearities of electrodynamic loudspeakers. These nonlinearities have become better and better known [5] [6] and some authors have proposed a new structure of loudspeaker with an ironless motor and without any outer rims and spider [7] in order to eliminate these nonlinearities.

The other drawback of an electrodynamic loudspeaker is that it is an time-varying system [8]. Indeed, the electrical resistance R_e increases in time due to the heat produced by the voice coil. Then, the compliance C_{ms} depends on time since the outer rim and the spider become more elastic because of the heat produced by the resistance. The Small signal model using lumped parameters does not forecast these time-varying phenomena, and such an time-varying analytic model taking into account these properties does not exist. In this paper, we put forward a way of characterizing experimentally the time dependence and the level dependence of the Small signal parameters. This experimental characterization allows us to compare two identical electrodynamic loudspeakers. One of them is supposed to be run in and the other one is not. The knowledge of the time necessary to break-in an electrodynamic loudspeaker is very important because this element of information gives indications about the physical properties of both the mechanical stiffness

²⁶ k and the mechanical damping parameter R_{ms} . The first section presents the
²⁷ Small signal model using lumped parameters and the main nonlinearities of
²⁸ an electrodynamic loudspeaker. The second section presents the experimental
²⁹ methodology to identify the variations of the Small signal parameters. In the
³⁰ third section, the time dependence of the Small signal parameters and its con-
³¹ sequences are discussed. The last section presents an analytical model which
³² takes into account the variations of the Small signal parameters in time and
³³ according to the input current.

³⁴ **2 The Small signal model using lumped parameters and its limits**

³⁵ *2.1 The Small signal model using lumped parameters*

³⁶ According to the Small signal model using lumped parameters, two cou-
³⁷ pled differential equations are necessary to describe the electrodynamic loud-
³⁸ speaker. One of them is called the electrical differential equation and is given
³⁹ by:

$$⁴⁰ \quad u(t) = R_e i(t) + L_e \frac{di(t)}{dt} + Bl \frac{dx(t)}{dt} \quad (1)$$

⁴¹ The other one is called the mechanical differential equation and is given by:

$$⁴² \quad M_{ms} \frac{d^2 x(t)}{dt^2} = Bl i(t) - R_{ms} \frac{dx(t)}{dt} - \frac{1}{C_{ms}} x(t) \quad (2)$$

⁴³ The parameters used in Eqs.(1) and (2) are the following:

⁴⁴ $i(t)$ =coil current [A]

⁴⁵ $u(t)$ =input voltage [V]

46 $x(t)$ =position of voice coil [m]

47 Bl =electrodynamic driving parameter [$T.m$]

48 R_{ms} =mechanical damping parameter and drag force [$N.s.m^{-1}$]

49 C_{ms} =mechanical compliance of suspension(spider, outer rim)[$m.N^{-1}$]

50 M_{ms} =equivalent mass of moving voice coil, cone, air[Kg]

51 R_e =electrical resistance of voice coil[Ω]

52 L_e =inductance of voice coil [H]

53 Eqs. (1) and (2) allow us to define the electrodynamic loudspeaker electrical
54 impedance Z_e which is expressed as follows:

55
$$Z_e = R_e + jL_e w + \frac{Bl^2}{R_{ms} + jM_{ms}w + \frac{1}{jC_{ms}w}} \quad (3)$$

56 Eq. (3) is well known and is often used to describe the electrodynamic loud-
57 speaker. However, Eq.(3) does not forecast the distortions created by an elec-
58 trodynamic loudspeaker and the time dependence of the Small signal parame-
59 ters. Moreover, if we take into account the eddy currents [9] which occur when
60 the input frequency increases, the electrical impedance Z_e should be written
61 as follows:

$$Z_e(i, t) = R_e(i, t) + \frac{jR_\mu(i, t)L_e(i, t)w}{jL_e(i, t)w + R_\mu(i, t)} + \frac{Bl(i, t)^2}{R_{ms}(i, t) + jM_{ms}(i, t)w + \frac{1}{jC_{ms}(i, t)w}} \quad (4)$$

62 where $R_\mu(i, t)$ is the eddy current resistance. $Z_e(i, t)$ is a time-varying nonlin-
63 ear transfer function; at each time and for different input currents, its value
64 changes. In Eq. (4), we assume all the parameters depend on both time and
65 input current. Strictly speaking, these dependences exist but it is very diffi-
66 cult to find them experimentally and to predict them analytically. All these

parameters have not the same sensitivity both to input current and to time. Moreover, some parameters vary a lot with the input current but do not create important distortions

2.2 Nonlinearities of electrodynamic loudspeakers

The nonlinearities that produce distortion phenomena can be classified into three categories. The first type corresponds to the motor nonlinearities and is described in section (2.2.1). The second type corresponds to the suspension nonlinearities and is described in section (2.2.4). The third type corresponds to the acoustical nonlinearities [10] and is not described here since these nonlinearities are not directly produced by the electrodynamic loudspeaker.

2.2.1 The motor structure

The force factor Bl is not uniform in the air gap. First, the force factor depends on the voice coil position. Indeed, the magnetic field induction B is the superposition of two fields. One of them is created by the permanent magnet and is time independent. This field crosses through the yoke pieces but only thirty per cents serves to move the coil. The other one is created by the coil and is time dependent. Klippel [3] proposed to model the force factor by using a polynomial writing.

$$Bl(x) = Bl_0 + Bl_1x + Bl_2x^2 \quad (5)$$

86 2.2.2 The voice coil inductance

87 The coil self inductance depends on the moving part position. This dependence
88 generates a reluctant force. This reluctant force is given by:

$$89 \quad F_{rel}(t) = \frac{1}{2}i(t)^2 \frac{dL_e(x)}{dx} \quad (6)$$

90 We see that when L_e does not depend on the voice coil position x , the reluctant
91 force $F_{rel}(t)$ equals zero, it is one of the assumptions of the Small signal model
92 using lumped parameters.

93 2.2.3 Eddy currents

94 The electrical conductivity of the iron is high enough to let the eddy currents
95 appear in the iron yoke pieces of the motor. Vanderkooy [9] proposed a model
96 which takes this phenomenon into account, the electrical impedance varies like
97 $L_e\sqrt{w}$. The interaction between the eddy currents and the current in the coil
98 generates a drag force F_{drag} which can be written as follows:

$$99 \quad F_{drag} = \eta(i, x) \frac{dx(t)}{dt}^{1,7} \quad (7)$$

100 where $\eta(i, x)$ can be defined as the sensitivity of the drag force according to
101 the eddy currents ; this one depends on input current and the position of the
102 voice coil.

103 2.2.4 The suspension

104 A classical suspension is mostly made of rubber, impregnated fabric or molded
105 plastic. The Small signal model using lumped parameters describes a suspen-

106 sion as an ideal spring but an actual suspension shows non linear behaviour.
 107 In consequence, its compliance C_{ms} depends on the movement amplitude and
 108 the induced damping parameter R_{ms} depends greatly on both the amplitude
 109 and frequency. More generally, many authors use the mechanical stiffness k
 110 which is defined by:

$$111 \quad k = \frac{1}{C_{ms}} \quad (8)$$

112 Like the force factor Bl , k can be written in terms of a polynomial function.

$$113 \quad k(x) = k_0 + k_1x + k_2x^2 \quad (9)$$

114 Such a model has been used by Klippel [3] to model the non linear behaviour
 115 of both the outer rim and the spider. However, such a model cannot take into
 116 account the effect of the hysteretic response of elastomers.

117 *2.3 Time varying properties of the electrodynamic loudspeakers*

118 *2.3.1 The electrical resistance R_e*

119 Many authors studied the non stationnarities of electrodynamic loudspeakers
 120 as M.Gander [11],[8] and showed that the Small signal parameters depend
 121 on time. The parameter which seems to be the most sensitive to time is the
 122 electrical resistance R_e . The electrical resistance R_e increases in time due to
 123 the heat produced by the coil:

$$124 \quad R_e(t) = \rho \frac{l}{S} (1 + \alpha \Delta T + \dots) \quad (10)$$

125 where $\alpha = 4.10^{-2}K^{-1}$ for the copper, l is the electric wire length, S is the
 126 electric wire cross section area and ΔT is the temperature elevation due to
 127 the heat produced by the coil. The electrical resistance variation can mod-
 128 ify both the outer rim and the spider properties. The heat produced by the
 129 electrical resistance due to the heat produced by the coil passes through to
 130 both the outer rim and the spider. Consequently, their temperature increases.
 131 The increase in the temperature of the spider and the outer rim generates a
 132 modification of their mechanical behaviour.

133 *2.3.2 Time dependence of the mechanical stiffness k*

134 Although analytical models taking into account the time dependence of the
 135 mechanical stiffness k do not exist, the properties of the outer rim change
 136 in time on account of the heat produced by the electrical resistance due to
 137 the Joule effect. Experimentally, this dependence is visible on the electrical
 138 impedance and this phenomenon is discussed in this paper. The outer rim and
 139 the spider exhibit both viscous and elastic characteristics. The type of vis-
 140 coelasticity which occurs in the case of an actual electrodynamic loudspeaker
 141 is non linear. In consequence, a volterra equation cannot be used to connect
 142 stress and strain and a simple model to describe such a behaviour does not ex-
 143 ist. Indeed, the outer rim deformations are large and the outer rim properties
 144 change under deformations.

145 **3 Improvement of the Small signal model using lumped param-** 146 **eters: experimental methodology**

147 *3.1 Introduction*

148 This section presents a way of deriving the time dependence and the input
149 current dependence of the Small signal parameters. For this purpose, an ex-
150 perimental way based on a measurement algorithm is described. The electro-
151 dynamic loudspeaker is characterized by the electrical impedance which, pre-
152 cisely measured, allows us to construct polynomial functions for each Small
153 signal parameter. The knowledge of the Small signal parameter variations al-
154 lows us to derive analytically the distortions created by the electrodynamic
155 loudspeaker.

156 *3.2 Principle of the measurement*

157 In order to measure the electrical impedance of a loudspeaker, it must be
158 placed in an anechoic chamber in a normalized plane. By varying the fre-
159 quency and the input current, we can measure the electrical impedance. So
160 as to increase the measurement precision when impedance variation is impor-
161 tant, different measurement algorithms have been developed. Basically, the
162 aim is to acquire more points when impedance variation is important and less
163 information when impedance tends to be constant with frequency.

164 3.3 *Measurement equipment and devices*

165 The electrical impedance is measured by a Wayne Kerr wedge that has an ex-
166 cellent precision ($10^{-4}\Omega$). Different algorithms are used to determine at which
167 frequencies impedance must be measured. Basically, points must be measured
168 when electrical impedance reaches a maximum or when impedance variation
169 with frequency is important. To do so, a dichotomic search of the maximum
170 impedance is used first to measure accurately the impedance near the reso-
171 nance frequency. The second algorithm is called in order to detect important
172 variation of impedance while the first algorithm is called to refine measurement
173 near impedance maxima.

174 3.4 *Determination of the Small signal parameters*

175 The Small signal parameters vary both in time and with the input current.
176 As it is very difficult to find the two dependences for each parameter, the
177 measurement algorithm is first used to derive the time dependence and after-
178 wards to derive the input current dependence. On the one hand, the input
179 current level is fixed and the electrical impedance is measured each time. On
180 the other hand, Thiele and Small variations in time are neglected and the
181 electrical impedance is measured for many input currents. In each case, we
182 work with three degrees of freedom. These three degrees of freedom are the
183 time t , the input current i and the frequency $f = \frac{\omega}{2\pi}$. The measured value is
184 always the electrical impedance Z_e .

185 3.5 Nonlinear parameter variations

186 To determine the nonlinear parameter variations, two impedance layers are
 187 used. One of them can be called the experimental impedance layer $Z_e^{(exp)}$ and
 188 is determined by using the measurement algorithm described in section (3).
 189 The other one can be called the theoretical impedance layer $Z_e^{(theo)}$ and is
 190 determined as follows: the Small signal parameters are assumed to vary with
 191 either the input current or time. In a first approximation, a polynomial writing
 192 is used to represent the dependence on the parameters with either the input
 193 current or time. The expansion is truncated after the 2nd term. Therefore, in
 194 the case of the input current dependence, we assume the electrical resistance
 195 R_e and R_μ to be constant; the Small signal parameters are expressed as follows:

$$196 \quad Bl(i) = Bl(1 + \mu_{Bl}i + \mu_{Bl}^2i^2) \quad (11)$$

$$197 \quad R_{ms}(i) = R_{ms}(1 + \mu_{R_{ms}}i + \mu_{R_{ms}}^2i^2) \quad (12)$$

$$198 \quad k(i) = k(1 + \mu_ki + \mu_k^2i^2) \quad (13)$$

$$199 \quad M_{ms}(i) = M_{ms}(1 + \mu_{M_{ms}}i + \mu_{M_{ms}}^2i^2) \quad (14)$$

$$200 \quad L_e(i) = L_e(1 + \mu_{L_e}i + \mu_{L_e}^2i^2) \quad (15)$$

201 and the electrical impedance becomes:

$$Z_{e1}^{(theo)}(i) = R_e + \frac{jR_\mu L_e(i)w}{jL_e(i)w + R_\mu} + \frac{Bl(i)^2}{R_{ms}(i) + jM_{ms}(i)w + \frac{k(i)}{jw}} \quad (16)$$

202 Again, in the case of the time dependence, we assume that R_μ is constant.
 203 The Small signal parameters are expressed as follows:

$$204 \quad R_e(t) = R_e(1 + \nu_{R_e}t + \nu_{R_e}^2t^2) \quad (17)$$

$$Bl(t) = Bl(1 + \nu_{Bl}t + \nu_{Bl}^2t^2) \quad (18)$$

$$R_{ms}(t) = R_{ms}(1 + \nu_{R_{ms}}t + \nu_{R_{ms}}^2t^2) \quad (19)$$

$$k(t) = k(1 + \nu_k t + \nu_k^2 t^2) \quad (20)$$

$$M_{ms}(t) = M_{ms}(1 + \nu_{M_{ms}}t + \nu_{M_{ms}}^2t^2) \quad (21)$$

$$L_e(t) = L_e(1 + \nu_{L_e}t + \nu_{L_e}^2t^2) \quad (22)$$

and the electrical impedance becomes:

$$Z_{e2}^{(theo)}(t) = R_e(t) + \frac{jR_\mu L_e(t)w}{jL_e(t)w + R_\mu} + \frac{Bl(t)}{R_{ms}(t) + jM_{ms}(t)w + \frac{k(t)}{jw}} \quad (23)$$

A least square method is used to identify all the parameters in the both cases ; this method is based on the Symplex algorithm. The principle of this algorithm is to minimize the difference ΔZ_e between the experimental impedance and the theoretical impedance. In the case of the time dependence of the Small signal parameters, this difference is expressed as follows:

$$\Delta Z_e^1(t) = \sum_{n=0}^{n=2} \left\| Z_e^{(exp)}(t) - Z_{e1}^{(theo)}(t) \right\|^2 \quad (24)$$

In the case of the input current dependence of the Small signal parameters, this difference is expressed as follows:

$$\Delta Z_e^2(i) = \sum_{n=0}^{n=2} \left\| Z_e^{(exp)}(i) - Z_{e2}^{(theo)}(i) \right\|^2 \quad (25)$$

When the algorithm converges, all the values describing the nonlinear parameters are obtained and allow us to predict analytically the distortions created by the electrodynamic loudspeaker by solving the time-varying nonlinear differential equation.

224 4 Time dependence of the Small signal parameters

225 This section describes a temporal study of two electrodynamic loudspeakers.
226 The electrodynamic loudspeakers used are two woofers (Eminence Alpha). One
227 of them is run in and the other one is not. First, the measurement algorithm
228 presented in the previous section is used in order to derive all the non-linear
229 parameters. Then, time-varying effects experimentally observed are discussed
230 and physically interpreted.

231 4.1 *Obtaining the experimental impedance*

232 The first step to derive the time dependence of the Small signal parameters
233 is to use the experimental impedance layer. As explained previously, the cur-
234 rent input current is fixed. A current which equals $i = 100mA$ is injected in
235 the electrodynamic loudspeaker. The electrodynamic loudspeaker used is sup-
236 posed to be run in. The lower measurement frequency equals $50Hz$ and the
237 upper measurement frequency equals $250Hz$. The experimental impedance is
238 measured for eight hours. Such an experimental impedance layer is represented
239 in Fig.(1). It can be noted that the time-varying effects are not visible in this
240 impedance layer but they are clearly shown in Figs.(2),(6) and (7).

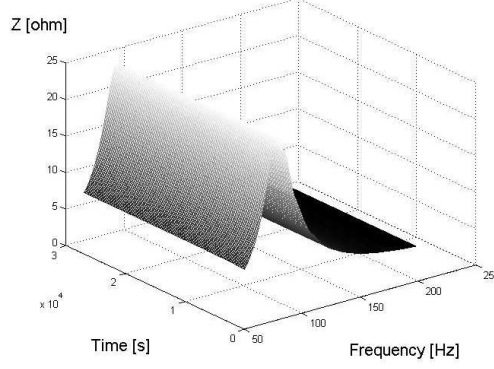


Fig. 1. Experimental three-dimensional representation of the electrical impedance modulus of the electrodynamic loudspeaker (x: time 0s to $3 \cdot 10^{-4}$ s) (y: 0Hz to 200Hz) (z: 0Ω to 25Ω)

241 4.2 Obtaining the parameters sensitive to time

242 4.2.1 Error sheet between the experimental impedance and the theoretical 243 impedance

244 In the previous section, the experimental impedance layer is determined with
245 the measurement algorithm presented in section (3). In this section, the experi-
246 mental impedance is compared to the theoretical one calculated with the Small
247 signal model using lumped parameters. For this purpose, the difference $\Delta Z_e^1(t)$
248 between the experimental impedance modulus and the theoretical impedance
249 modulus is calculated for each frequency and at each time. This difference
250 $\Delta Z_e^1(t)$ is represented in Fig.(2). The mean difference $\overline{\Delta Z_e}$ is defined as the
251 difference $\Delta Z_e^1(t)$ divided by the number of points necessary to plot the ex-
252 perimental impedance layer. By using the Small signal model using lumped
253 parameters with constant parameters, the mean difference $\overline{\Delta Z_e}$ equals 0, 20Ω .

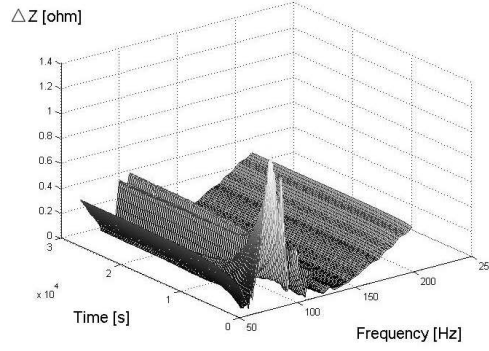


Fig. 2. Three-dimensional representation of the difference $\Delta Z_e^1(t)$ between the experimental impedance and the theoretical impedance ; the theoretical impedance is based on the Small signal model using lumped parameters with constant parameters (x: time 0s to $3 \cdot 10^4$ s) (y: 0Hz to 200Hz) (z: 0Ω to 25Ω)

4.2.2 Parameter sensitive to time

To reduce $\overline{\Delta Z_e}$, we use the Symplex algorithm and the parameter which is the most sensitive to time is the equivalent mechanical stiffness k . As a remark, although the electrical resistance of the voice coil R_e increases in time, its time variation is less important than the mechanical stiffness one. Moreover, the variations of the other Small signal parameters are not so important as the mechanical stiffness variation. In Fig.(3), we represent the difference $\Delta Z_e^1(t)$ between the experimental impedance modulus and the theoretical impedance modulus which takes into account the time variation of the mechanical stiffness k . This difference is a function of both time and frequency. The impedance layer is zoomed for more legibility. The temporal axe varies from 0s to 200s. The mean difference $\overline{\Delta Z_e}$ equals $0,19\Omega$. The figure (4) shows the relative mechanical stiffness as a function of time ($k_0 = 3714N/m$). The mechanical stiffness k decreases in time since heat produced by the electrical resistance passes through to the outer rim and modifies its properties. The increasing temperature is one factor contributing to the deformation of the outer rim,

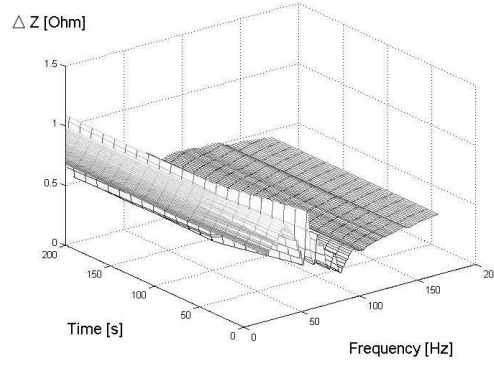


Fig. 3. Three-dimensional representation of the difference between the experimental impedance and the theoretical impedance ; the theoretical impedance is based on Small signal model using lumped parameters with variable mechanical stiffness (x: time 0s to 3.10^4 s) (y: 0Hz to 200Hz) (z: 0Ω to 25Ω)

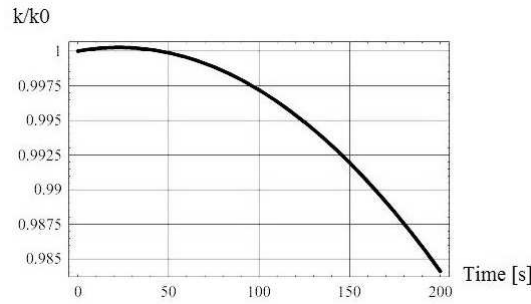


Fig. 4. The relative mechanical stiffness is a function of time [s]

and viscoelastic properties change with decreasing or increasing temperature.

4.3 Resonance frequency variation

Another interesting temporal effect is the resonance frequency variation. It is quite difficult to obtain the resonance frequency experimental measurement in time because its variation is very fast and the time necessary to get the measurement points by the algorithm is only about half a second. Fig.(5) shows the resonance frequency f_{res} as a function of time. We see in this figure

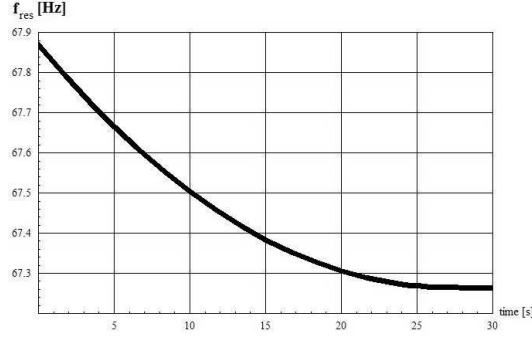


Fig. 5. The resonance frequency [Hz] is a function of time [s]

that the resonance frequency decreases in time. This effect can be explained since the mechanical stiffness of suspension (spider, outer rim) depends on time. In consequence, the resonance frequency is not constant and depends also on time. In short, the decrease in mechanical stiffness generates the decrease in the resonance frequency.

$$f_{res}(t) = \frac{1}{2\pi} \sqrt{\frac{k - k_3 t - k_4 t^2}{M m s}} \quad (26)$$

4.4 Comparison between two loudspeakers: one of them is not run in and the other one is

This section presents an experimental comparison between two electrodynamic loudspeakers. One of them is supposed to be run in and the other one is not. The electrodynamic loudspeaker which is run in has been used for one year. In consequence, its mechanical properties have changed, particularly for the outer rim and the spider which have become both more elastic and worn. For five hours, we measured continually the electrical impedance of the two electrodynamic loudspeakers. The experimental electrical impedance modulus $Z_e(t)$ of the electrodynamic loudspeaker which is not run in is represented in Fig.(6). As said previously, $Z_e(t)$ is plotted at different instants and is a func-

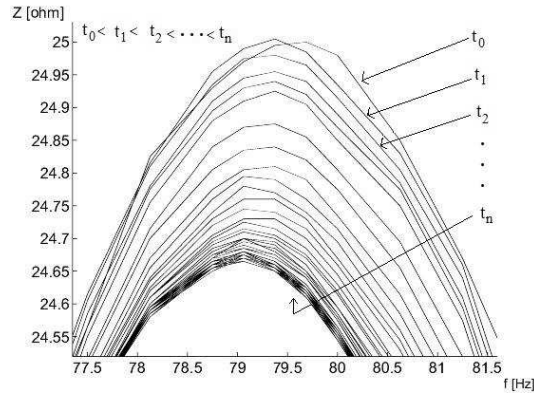


Fig. 6. Electrical impedance modulus of the woofer which is not run in. The electrical impedance modulus $[\Omega]$ is a function of frequency $[\text{Hz}]$ and is plotted at different instants around the resonance frequency.

tion of frequency. In this figure, we see that the electrical impedance decreases in time and it is mainly due to the change of the mechanical properties. Another interesting point is that the resonance frequency varies quickly in time between t_0 and t_1 which corresponds to 8 seconds. This variation is probably due to the dry friction behaviour of the outer rim.

Fig. (7) represents the electrical impedance modulus of the electrodynamic loudspeaker which is supposed to be run in. As in the previous case, $Z_e(t)$ is plotted at different instants and is a function of frequency. This figure shows that the decrease in electrical impedance modulus is less important for the woofer which is run in than the one which is not. This diminution is about $0,4\Omega$ for the woofer which is not run in, whereas this diminution is $0,05\Omega$ for the woofer which is run in. Moreover, the resonance frequency variation is less important for the woofer which is run in than the one which is not. This resonance frequency variation is about 1Hz for the woofer which is not, whereas this variation is $0,4\text{Hz}$ for the woofer which is run in. Furthermore, the resonance frequency is very different between the two loudspeakers although they

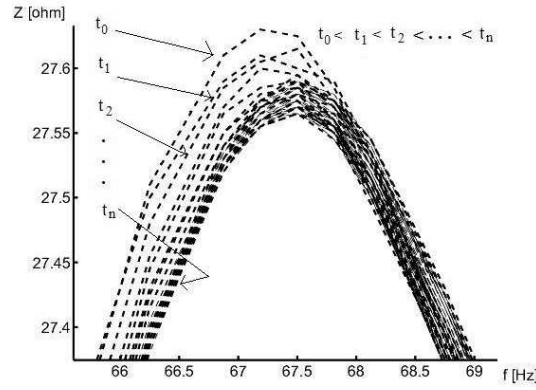


Fig. 7. Electrical impedance modulus of the woofer which is run in. The electrical impedance modulus $[\Omega]$ is a function of frequency $[Hz]$ and is plotted at different instants around the resonance frequency.

are both the same. The resonance frequency of the woofer which is run in is about $67Hz$ whereas the resonance frequency of the woofer which is not run in is about $79Hz$. This resonance frequency discrepancy is probably due to the fabrication scattering and the change in time of the membrane mechanical properties.

4.5 Electrical impedance variation in time

The previous section shows that the electrical impedance varies in time. The aim of this section is to show that the electrical impedance does not vary in the same way according to the frequency measurement. For this purpose, we plot the electrical impedance for the two loudspeakers at two different fixed frequencies. One of them is at the resonance frequency and the other one is at $200Hz$. In Fig. (8), the electrical impedance modulus of the woofer which is run in is a function of time. The fixed frequency equals $200Hz$ and the input current equals $100mA$. This figure shows that the electrical impedance modulus increases in time. In Figure (9), we still plot the electrical impedance modulus

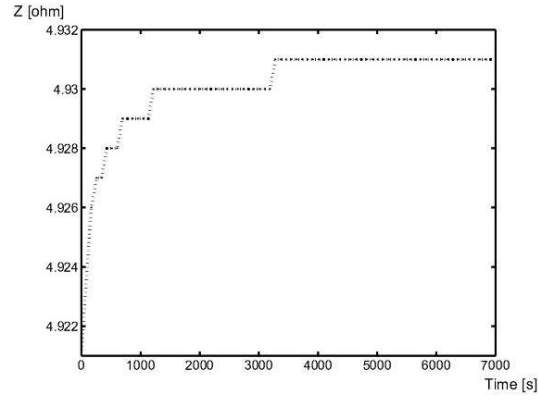


Fig. 8. Electrical impedance modulus of the woofer which is run in. The frequency equals $200Hz$ and the input current equals $100mA$. The electrical impedance modulus is a function of time.

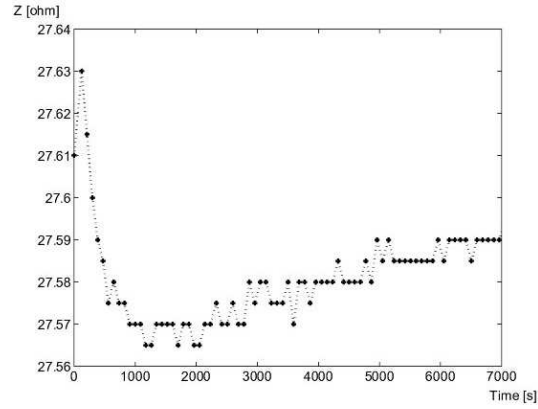


Fig. 9. Electrical impedance modulus of the boomer which is run in. The frequency equals the resonance frequency and the input current equals $100mA$. The electrical impedance modulus is a function of time.

325 of the woofer which is run in, but the fixed frequency equals the resonance
 326 frequency. The temporal behaviour of the electrical impedance is very different
 327 according to the frequency measurement. Actually, the electrical impedance of
 328 the woofer which is run in decreases a lot at the beginning and increases only
 329 after three hour measurement. Moreover, the electrical impedance modulus
 330 varies more in time at the resonance frequency than another frequency (here:
 331 $200Hz$).

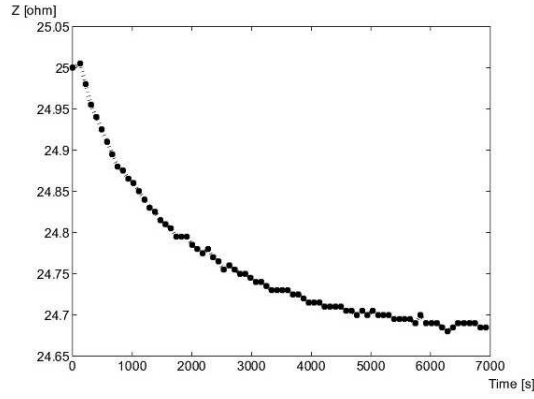


Fig. 10. Electrical impedance modulus of the woofer which is not run in. The frequency equals the resonance frequency and the input current equals $100mA$. The electrical impedance modulus is a function of time

332 The same experimental measurements are done with the electrodynamic loud-
 333 speaker which is not run in. Again, an experimental measurement is realized
 334 with a fixed frequency which equals the resonance frequency. Such an experi-
 335 mental measurement is represented in Fig.10 This figure shows that the elec-
 336 trical impedance decreases in time. The behavior of the electrical impedance
 337 is very different according to the electrodynamic loudspeaker used at the res-
 338 onance frequency. The figure (10) shows the electrical impedance modulus of
 339 the woofer which is not run in as a function of time. The fixed frequency equals
 340 $200Hz$ and the input current equals $100mA$.

341 As seen previously in the case of the run in electrodynamic loudspeaker, the
 342 electrical impedance modulus increases in time. In Fig.(11), the electrical
 343 impedance modulus decreases in time. Moreover, we see that the electrical
 344 impedance modulus varies more at the resonance frequency than another fre-
 345 quency (here: $200Hz$).

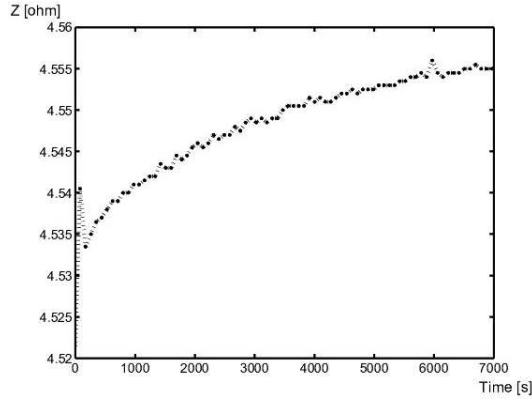


Fig. 11. Electrical impedance modulus of the woofer which is not run in. The frequency equals $200Hz$ and the input current equals $100mA$. The electrical impedance modulus is a function of time.

346 4.6 Running in an electrodynamic loudspeaker

347 The aim of this section is to show the time necessary to consider that an
 348 electrodynamic loudspeaker is run in. For this purpose, we use the electrical
 349 impedance modulus of the electrodynamic loudspeaker. We take a frequency
 350 which equals the resonance frequency, an input current which equals $100mA$
 351 and we plot the electrical impedance modulus at each instant. Such an elec-
 352 trical impedance modulus is plotted in Fig.(12). This figure shows that the
 353 electrical impedance modulus does not vary after 10^4s , which corresponds to
 354 about three hours. It can be concluded that this is the time necessary for
 355 breaking in this electrodynamic loudspeaker.

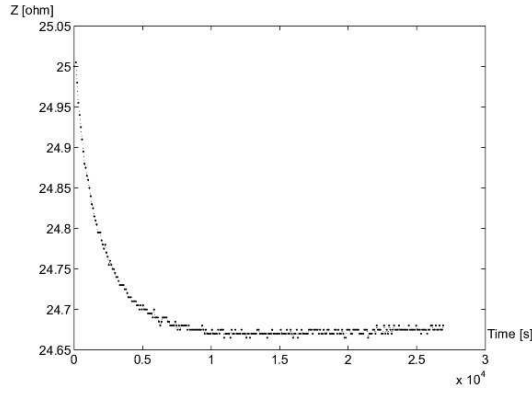


Fig. 12. Electrical impedance modulus of the woofer which is not run in. The frequency equals the resonance frequency and the input current equals $100mA$. The electrical impedance modulus is a function of time.

5 Analytical study of the distortions created by an electrodynamic loudspeaker

5.1 Obtaining the experimental impedance

The way of obtaining the experimental impedance is similar to the one described previously. In order to derive the input current dependence of Small signal parameters, the first step is to use the experimental impedance layer. The time dependence of Small signal parameters is neglected and the input current varies from $20mA$ to $200mA$. The Wayne Kerr wedge cannot deliver currents higher than $200mA$. The electrodynamic loudspeaker used is supposed to be run in. The lower measurement frequency equals $50Hz$ and the upper measurement frequency equals $650Hz$. The experimental impedance layer is represented in Fig.(13).

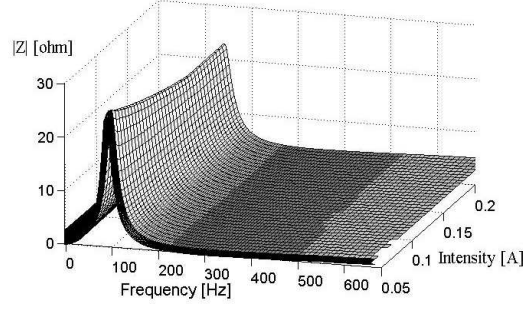


Fig. 13. Experimental three-dimensional representation of the electrical impedance modulus of the electrodynamic loudspeaker (x:0.05A to 0,2A) (y: 0Hz to 650Hz) (z: 0Ω to 25Ω)

368 5.2 Obtaining the parameters sensitive to the input current

369 5.2.1 Error sheet between the experimental impedance and the theoretical 370 impedance

371 In the previous section, the experimental impedance layer is determined with
372 the measurement algorithm presented in section (3). In this section, the experi-
373 mental impedance is compared to the theoretical one calculated with the Small
374 signal model using lumped parameters. For this purpose, the difference $\Delta Z_e^2(i)$
375 between the experimental impedance modulus and the theoretical impedance
376 modulus is calculated for each frequency and at each intensity. The intensity
377 step is 10mA. This difference $\Delta Z_e^2(i)$ is represented in Fig.(14). We define
378 the mean difference $\overline{\Delta Z_e}$ as the difference $\Delta Z_e^2(i)$ divided by the number of
379 points necessary to plot the experimental impedance layer. By using the Small
380 signal model using lumped parameters with constant parameters, the mean
381 difference $\overline{\Delta Z_e}$ equals 2,04Ω.

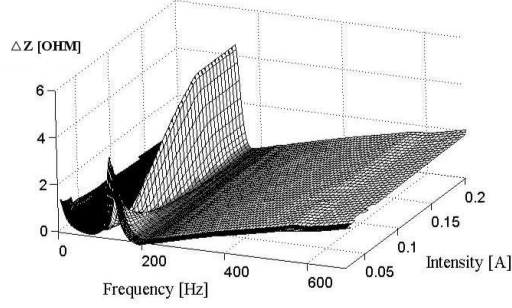


Fig. 14. Three-dimensional representation of the difference $\Delta Z_e^2(i)$ between the experimental impedance and the theoretical impedance ; the theoretical impedance is based on the Small signal model using lumped parameters with constant parameters (x:0,05A to 0,2A) (y: 0Hz to 200Hz) (z: 0Ω to 6Ω)

5.2.2 Parameters sensitive to the input current

To reduce $\overline{\Delta Z_e}$, the Symplex algorithm is used and five nonlinear parameters are taken into account to reduce $\overline{\Delta Z_e}$. In Fig.(15), we represent the difference $\Delta Z_e^2(i)$ between the experimental impedance modulus and the theoretical impedance modulus which takes into account the Small signal parameter variations. This difference is a function of both the input current and frequency. The mean difference $\overline{\Delta Z_e}$ equals 0,39Ω.

In table (1), all the parameters and their expansions are described and the sensitivity to the least square is precise. This table shows that the parameter which is the more sensitive to the input current is the equivalent damping parameter R_{ms} .

5.3 Obtaining the time-varying nonlinear differential equation

This section presents the time-varying nonlinear differential equation of the electrodynamic loudspeaker which is run in. For this purpose, we take into

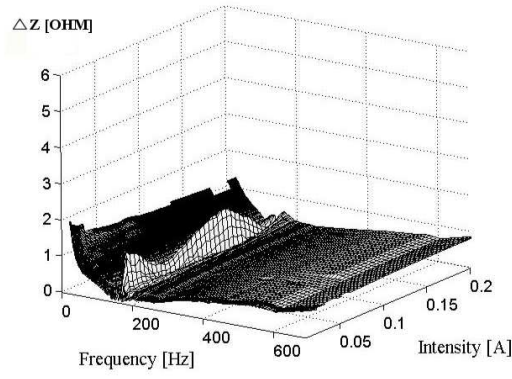


Fig. 15. Three-dimensional representation of the difference between the experimental impedance and the theoretical impedance ; the theoretical impedance is based on the Small signal model using lumped parameters with variable parameters (x: 0A to 0,2A) (y: 0Hz to 200Hz) (z: 0Ω to 25Ω)

Ranking	Parameter	Law of variation	$\overline{\Delta Z_e}[\Omega]$	Sensitivity
1	R_{ms}	$1.1(1 + 4.09i - 8.36i^2)$	1.24	33%
2	Bl	$5.5(1 + 0.33i - 1.02i^2)$	1.67	18%
3	M_{ms}	$0.009(1 + 0.56i - 0.22i^2)$	1.74	14%
4	k	$7440(1 - 0.2i + 0.9i^2)$	1.86	8%
5	L_e	$0.0017(1 - 1.68i + 7.58i^2)$	1.98	3%
6	R_μ	2, 28	2.04	0%
7	R_e	3, 17	2.04	0%

Table 1

Ranking of the parameters according to their sensitivity to the least square algorithm

account the nonlinear parameters defined in the previous section and we also take into account the time variation of the mechanical stiffness k . The time-varying nonlinear differential equation is defined by Eq.(27) in the case when we also take into account the variation of the electrical resistance R_e in time.

$$a(i) \frac{d^3 x(t)}{dt^3} + b(i, t) \frac{d^2 x(t)}{dt^2} + c(i, t) \frac{dx(t)}{dt} + d(i, t)x(t) = u(t) \quad (27)$$

with

$$a(i) = \frac{(Mms(1 + \mu_{Mms}i + \mu_{Mms}^2 i^2))(Le(1 + \mu_{Le}i + \mu_{Le}^2 i^2))}{Bl(1 + \mu_{Bl}i + \mu_{Bl}^2 i^2)} \quad (28)$$

$$b(i, t) = \frac{((Mms(1 + \mu_{Mms}i + \mu_{Mms}^2 i^2)R_e(1 + \nu_{Re}t + \nu_{Re}^2 t^2))}{Bl(1 + \mu_{Bl}i + \mu_{Bl}^2 i^2)} + \frac{R_{ms}(1 + \mu_{Rms}i + \mu_{Rms}^2 i^2)L_e(1 + \mu_{Le}i + \mu_{Le}^2 i^2)}{Bl(1 + \mu_{Bl}i + \mu_{Bl}^2 i^2)} \quad (29)$$

403

$$c(i, t) = \frac{R_e(1 + \nu_{Re}t + \nu_{Re}^2 t^2)(Rms(1 + \mu_{Rms}i + \mu_{Rms}^2 i^2))}{Bl(1 + \mu_{Bl}i + \mu_{Bl}^2 i^2)} + \frac{(Le(1 + \mu_{Le}i + \mu_{Le}^2 i^2))k(1 + \nu_k t + \nu_k^2 t^2)(1 + \mu_k i + \mu_k^2 i^2)}{Bl(1 + \mu_{Bl}i + \mu_{Bl}^2 i^2)} + \frac{(Bl(1 + \mu_{Bl}i + \mu_{Bl}^2 i^2))^2}{Bl(1 + \mu_{Bl}i + \mu_{Bl}^2 i^2)} \quad (30)$$

$$d(i, t) = \frac{R_e(1 + \nu_{Re}t + \nu_{Re}^2 t^2)(k(1 + \nu_k t + \nu_k^2 t^2)(1 + \mu_k i + \mu_k^2 i^2))}{Bl(1 + \mu_{Bl}i + \mu_{Bl}^2 i^2)} \quad (31)$$

5.4 Solving the time-varying nonlinear differential equation

We explain here how to solve the equation defined in the previous section. We can point out that the coefficient $a(i)$ defined in Eq.(28) is the only coefficient which is constant in time. We use the notation Re_t and k_t to indicate that these

parameters depend on time. To solve the time-varying nonlinear differential equation, a Taylor series expansion is used.

5.4.1 Discussion about the time-varying differential equation

It is noticeable that the temporal variations of the Small signal parameters do not create any important distortions. Indeed, if we assume all the Small signal parameters to be constant with the input current, the general differential equation of the electrodynamic loudspeaker is written:

$$\tilde{a} \frac{d^3 x(t)}{dt^3} + \tilde{b}(t) \frac{d^2 x(t)}{dt^2} + \tilde{c}(t) \frac{dx(t)}{dt} + \tilde{d}(t)x(t) = u(t) \quad (32)$$

with

$$\tilde{a} = \frac{M_{ms} L_e}{Bl} \quad (33)$$

$$\tilde{b}(t) = \frac{M_{ms} R_e (1 + \nu_{R_e} t + \nu_{R_e}^2 t^2)}{Bl} + \frac{R_{ms} L_e}{Bl} \quad (34)$$

$$\tilde{c}(t) = \frac{R_e (1 + \nu_{R_e} t + \nu_{R_e}^2 t^2) R_{ms} + Bl^2 + k(1 + \nu_k t + \nu_k^2 t^2) L_e}{Bl} \quad (35)$$

$$\tilde{d}(t) = \frac{k(1 + \nu_k t + \nu_k^2 t^2) R_e (1 + \nu_{R_e} t + \nu_{R_e}^2 t^2)}{Bl} \quad (36)$$

The time-varying differential equation defined in Eq.(32) is a hypergeometric equation and can be solved in the general case by using the theory of the Power Series Method [12]. However, if we take $u(t) = Ae^{j\omega t}$ where A is a term of amplitude, the response does not contain terms in $e^{j2\omega t}, e^{j3\omega t}, \dots$. In consequence, we deduct that the time dependence of the Small signal parameters does not generate any distortions.

428 5.5 Solving the nonlinear differential equation

429 The nonlinear differential equation can be solved at each time. By assuming
 430 the electrical resistance to be constant in time, the only parameter sensitive to
 431 time is the mechanical stiffness. To simplify the resolution of the time-varying
 432 nonlinear differential equation, we can write that at each time, the nonlinear
 433 differential equation is stationary. The distortions predicted by the nonlinear
 434 differential equation depend on time but can be solved at each time. The
 435 study of the nonlinear small signal parameters can be done with either the
 436 input current or with the position of voice coil. In fact, the relation between
 437 the input current i and the position $x(t)$ of the voice coil is linear. Indeed,
 438 by using the classical approach, Laplace Law describes the movement of the
 439 voice coil at first order.

$$440 \quad M_{ms} \frac{d^2 x(t)}{dt^2} = Bli(t) \quad (37)$$

441 If we consider that the current is varying sinusoidally in time, above the fre-
 442 quency resonance, the displacement of the voice coil is proportional to the
 443 Laplace force and in opposed directions. The displacement of the voice coil
 444 can be described by:

$$445 \quad x = -\frac{Bli}{M_{ms}w^2} \quad (38)$$

446 where w is the radian frequency of the input current. In consequence, it exists
 447 a parameter α which verifies:

$$448 \quad x = \alpha i \quad (39)$$

where $\alpha = -\frac{Bl}{M_{ms}w^2}$. All the Small signal parameters can be expressed as a Taylor series expansion. By inserting all these expansion series in Eq.(28), we obtain a classical nonlinear differential equation. Its solution is given by Eq.(40). The solution is developed until the order 2 (μ_2).

$$x(t) = x_0(t) + \mu x_1(t) + \mu^2 x_2(t) + \dots \quad (40)$$

where $x_0(t)$ is the solution of the nonlinear differential equation of the electrodynamic loudspeaker when the terms with orders higher than zero are neglected, $x_1(t)$ is the solution of the nonlinear differential equation when the terms with orders higher than one and smaller than one are neglected, $x_2(t)$ is the solution of the nonlinear differential equation when the terms with orders higher than two and smaller than two are neglected. In short, the solution of the nonlinear differential equation of the electrodynamic loudspeaker is given by:

$$x(t) = A \cos(wt) + B \sin(wt) + C \cos(2wt) + D \sin(2wt) + \dots \quad (41)$$

The terms A and B can be found by inserting $A \cos(wt) + B \sin(wt)$ in Eq.(27) with an excitation $u(t)$ which equals $P \sin(wt)$ where P is an amplitude. The terms C and D can be found by taking the terms with orders higher than one and smaller than one into account, etc...

5.6 Experimental and theoretical displacement spectrums

This section presents the experimental and the theoretical displacement spectrums of the electrodynamic loudspeaker which is run in. The theoretical displacement spectrum is obtained by calculating the Fourier transform of the

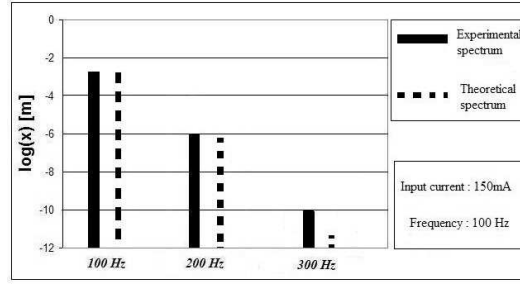


Fig. 16. Experimental and theoretical spectrums of the electrodynamic loudspeaker which is run in. The input current equals $100mA$ and the input frequency equals $100Hz$.

471 solution given in Eq.(41). The experimental displacement spectrum is obtained
 472 by using a laser Doppler velocimeter. The theoretical displacement spectrum is
 473 consistent with the experimental displacement spectrum. The theoretical and
 474 experimental first-harmonic and second-harmonic shows a very good agree-
 475 ment. However, the theoretical third-harmonic is lower than the experimental
 476 one. This discrepancy between the theoretical third-harmonic and the exper-
 477 imental one shows the limit of the use of a series Taylor expansion. It can be
 478 noted that the experimental spectrums have been measured at low frequen-
 479 cies. For higher frequencies, the theoretical model should take into account
 480 membrane modes.

481 6 Conclusion

482 The aim of this paper is the study of the time-varying effects and nonlinear ef-
 483 fects of electrodynamic loudspeakers. A temporal study based on a very precise
 484 measurement shows the time dependence of the membrane mechanical stiffness
 485 k . However, this time dependence does not create any distortions. Moreover,
 486 two identical electrodynamic loudspeakers are compared and important time

487 discrepancies are discussed. The resonance frequency between an electrody-
488 namic loudspeaker which is run in and one which is not is extremely different
489 and does not vary in time in the same way. Then, the time-varying nonlinear
490 differential equation of the electrodynamic loudspeaker is solved by using a se-
491 ries Taylor expansion. For this purpose, the time-varying effects are neglected
492 but can be taken into account by solving the nonlinear differential equation
493 at different instants. The theoretical displacement spectrum is consistent with
494 the experimental displacement spectrum.

References

- [1] R. H. Small, "Closed-box loudspeaker systems, part 1: Analysis," *J. Audio Eng. Soc.*, vol. 20, pp. 798–808, 1972.
- [2] A. J. M. Kaizer, "Modeling of the nonlinear response of an electrodynamic loudspeaker by a volterra series expansion," *J. Audio Eng. Soc.*, vol. 35, pp. 421–433, June 1987.
- [3] W. Klippel, "Dynamic measurement and interpretation of the nonlinear parameters of electrodynamic loudspeakers," *J. Audio Eng. Soc.*, vol. 38, pp. 944–955, 1990.
- [4] W. Klippel, "Loudspeaker nonlinearities - cause, parameters, symptoms," *J. Audio Eng. Soc.*, vol. 54, pp. 907–939, 2006.
- [5] J. W. Noris, "Nonlinear dynamical behavior of a moving voice coil," in *105th convention, San Francisco*, no. 4785, Audio Eng. Soc., 1998.
- [6] C. S. A. Dobrucki, "Nonlinear distortions of woofers in fundamental resonance region," in *80th convention, Montreux*, no. 2344, Audio Eng. Soc., 1986.

- [7] M. Berkouk, “Contribution a l’etude des actionneurs electrodynamiques.” These de doctorat de l’Universite de Bretagne Occidentale, 2001.
- [8] M. R. Gander, “Dynamic linearity and power compression in moving-coil loudspeaker,” *J. Audio Eng. Soc.*, pp. 627–646, September 1986.
- [9] J. Vanderkooy, “A model of loudspeaker driver impedance incorporating eddy currents in the pole structure,” *J. Audio Eng. Soc.*, vol. 37, pp. 119–128, March 1989.
- [10] G. Lemarquand and M. Bruneau, “Large bandwidth loudspeaker emitting coherent acoustic waves: nonlinear inter-modulation effects,” *J. Audio Eng. Soc.*, 2007.
- [11] M. R. Gander, “Moving-coil loudspeaker topology as an indicator of linear excursion capability,” *J. Audio Eng. Soc.*, vol. 29, 1981.
- [12] E. Kreyszig, *Advanced Engineering Mathematics*. Willey, 2006.